Characterization of Biochar Obtained by Co-Pyrolysis of Waste Newspaper with High-Density Polyethylene

Weimin Chen, Minzhi Chen, and Xiaoyan Zhou*

The pyrolysis of waste newspaper (WP) and co-pyrolysis of waste newspaper with high-density polyethylene (HDPE) (1:1 wt%) were carried out in a quartz tube at 500 °C to obtain biochars. The biochars were characterized in detail by X-ray diffraction (XRD), thermogravimetric analysis (TG), Fourier transform infrared spectroscopy (FT-IR), X-ray photoelectron spectroscopy (XPS), elemental analysis, scanning electron microscopy (SEM), automated specific surface area and pore size analyzer, and Raman spectroscopy to determine their physical and chemical properties. The analysis results for WP/HDPE-derived biochar (CWH) were compared to WP-derived biochar (CWB). The CWH had lower oxygen-containing groups, increased aromatic structure, higher calorific value, higher fuel ratio, and greater porosity development. CWH is more appropriate as solid fuel, soil adsorbent, or activated carbon precursor as compared to CWB.

Keywords: Co-pyrolysis; Waste newspaper; High-density polyethylene; Biochar; Oxygen-containing groups; Aromatic structure

*Contact information: College of Materials Science and Engineering, Nanjing Forestry University, Nanjing 210037, China; *Corresponding author: zhouxiaoyan@njfu.edu.cn*

INTRODUCTION

The annual worldwide production of municipal solid waste (MSW) in China has reached almost two hundred million tons and is increasing at 10% per year. Waste newspaper and waste plastic account for about 15% and 10% of MSW, respectively. Traditional recycling processes for MSW, such as landfill, compost, and incineration, cannot fundamentally solve the environmental and green energy recycling issues.

Pyrolysis techniques have received much attention in recent years because these new techniques can convert MSW such as paper, fabric, rubber, plastic, and sawdust into high-value feedstocks, including pyrolysis gases, bio-oils, and biochars (Mckendry 2002; Czernik and Bridgwater 2004; Mohan *et al.* 2006). Pyrolysis techniques not only can reduce the volume of MSW, but also can recover chemicals and convert them into clean fuels in place of non-renewable fossil fuels.

Biochar is produced by slow or fast biomass pyrolysis, and almost all carbonaceous biomass can be converted into biochar. Previous studies have demonstrated that biochar has beneficial effects on soil microbial activity, soil fertility, nutrient availability, and reduction of greenhouse gas emissions (Bornermann *et al.* 2007; Steinbeiss and Gleixner 2009). Iron-supported biochar can be used as an effective catalyst for tar cracking, which can coke downstream reforming, upgrading, and fuel cell catalysts during biomass gasification and pyrolysis (Sutton *et al.* 2001).

Biochar also can be used as a bio-composite constituent in such materials as plastic-biochar composite, rubber-biochar composite, and wood plastic-biochar composite (Ahmetli *et al.* 2004). Because of its low oxygen content, biochar can be used as a solid fuel. Biochar obtained by corn cob pyrolysis can be used as a fuel for direct carbon fuel cells employing a composite electrolyte composed of samarium-doped ceria and a eutectic carbonate phase (Yu *et al.* 2014). It should be noted that about 80% of all crop and forestry residues may be converted to biochar and energy by the year 2050, as estimated by the International Biochar Initiative Organization.

In recent years, co-processing technologies such as co-gasification, co-combustion, co-firing, and co-pyrolysis have been studied to produce bio-fuels, which can replace non-renewable fossil fuels. In particular, co-pyrolysis allows researchers to observe and interpret whether any synergistic effects occurred during the process (Suelves *et al.* 2002; Vasile and Brebu 2006; Rotliwala and Parikh 2011). Co-pyrolysis techniques also could solve the issues associated with the fact that different components of MSW are not easily separated from the post-consumer stream. Synthetic polymers could act as hydrogen sources in thermal co-pyrolysis with organic natural materials with less hydrogen content such as biomass or coal. Plastics could potentially be a beneficial feedstock because of their higher hydrogen content and the small amount of water in their pyrolysis-derived oil (Achilias *et al.* 2007). Therefore, co-pyrolysis of waste newspaper with waste high-density polyethylene could balance the carbon, oxygen, and hydrogen in the feedstock, with strong effects on the properties of degradation products such as biochar.

In this study, the biochar obtained by co-pyrolysis was characterized in detail to determine its physical and chemical properties. Such understanding is essential for development of co-pyrolysis biochar applications and technology for the production of industrial wastes with improved value.

EXPERIMENTAL

Materials

The feedstock used in this study included waste newspaper (WP) and high-density polyethylene (HDPE). WP was obtained from a local newsstand, milled, and sieved to a particle size of less than 1 mm, and dried for 24 h at 80 °C. HDPE obtained from local factory was milled to a particle size of less than 500 μm and dried for 8 h at 60 °C. The mass ratio of the WP/HDPE blend was 1:1, and it was homogenized by mixing and subsequent rolling for 12 h.

Methods

Pyrolysis process and biochar preparation

The pyrolysis experiments were established as seen in Fig. 1 under a 20 mL/min N_2 flow. Approximately 6 g of feedstock material was used for each experiment and heated up to the final decomposition temperature of 500 °C at 10 °C /min. The WP-derived biochar (CWB) and WP/HDPE blend-derived biochar (CWH) were obtained from the crucible after pyrolysis was finished.

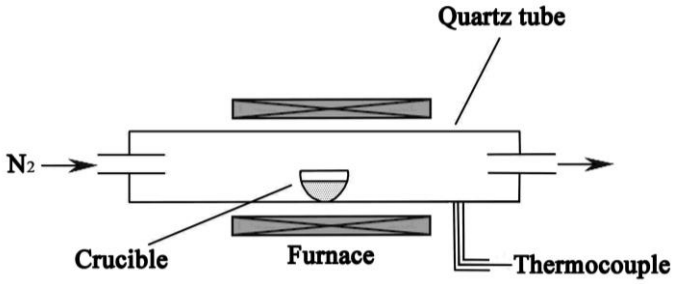

Fig. 1. Pyrolysis procedure for WP, HDPE, and WP/HDPE blend

Characterization methods

X-ray diffraction (XRD) was carried out for crystal structure analysis in an Ultima-IV (Rigaku Corporation, Japan) using Cu Kα radiation (40 kV, 200 mA) and a 2θ value ranging from 5 ° to 85 ° with a step size of 0.02 °/s.

Thermogravimetric analysis (TG) was performed in a Netzsch STA449C analyzer (Netzsch GmbH, Germany). A total of 5 to 10 mg of sample was heated up to 800 °C under a 20 mL/min N_2 flow at the rate of 10 °C /min.

Fourier transform infrared spectroscopy (FT-IR) was used for chemical structure analysis in a Nexus870 (Nicolet, USA) using a KBr disc containing 1% samples. Sixteen scans were conducted for each sample in the range from 4000 to 400 cm^{-1}, with a resolution of 4 cm^{-1}. The precision was no more than 0.01 cm^{-1}.

Elemental analysis was carried out to determine the relative contents of C, H, and O in a CHN-O-Rapid analyzer (Heraeus, Gemany). Only averaged values over four repeated analysis were considered to compensate for the eventual heterogeneity of the sample. The H/C and O/C atomic ratios were calculated from these elemental analysis data. Calorific value was measured in an adiabatic oxygen bomb calorimeter (Parr Co., USA). About 0.2 g of the dried sample was conducted in the calorimeter to measure the constant volume heat released by the combustion with pure oxygen.

The surface morphology of the samples was studied using a scanning electron microscope (FEI Co., USA). All samples were first quenched in liquid nitrogen for 5 min, cleaved, and coated with fine film (5 nm) of gold palladium using PECS coating machine (Gatan Inc., USA) to reduce charging effects.

Pore properties of biochars were characterized in an automated surface area and pore size analyzer (Micromeritics Co., USA). The nitrogen adsorption isotherms were obtained at 77 K. The Brunauer-Emmett-Teller (BET) standard method was applied to obtain the BET surface area. Total pore volume was calculated by converting the amount of nitrogen gas adsorbed at a relative pressure of 0.99 to the volume of liquid adsorbed. Micropore volume was calculated by *t*-plot method.

X-ray photoelectron spectroscopy (XPS) was used to examine the surface chemical structure in an AXIS UltraDLD (Shimadzu, Japan). Low-resolution spectra from 0 to 1100 eV and high-resolution spectra of the C1s region from 280 to 300 eV were recorded with a pass energy of 10 eV and non-monochromatic Mg Kα and Al Kα X-radiations ($h\gamma$ = 1253.7 eV and 1486.7 eV, respectively). The C1s peaks were deconvoluted into four components (C1, C2, C3, and C4).

Raman spectroscopy was performed in a DXR532 (Nicolet, USA). The source of radiation was a laser operating at a wavelength of 532 nm. Biochar powders were prepared for analysis under the laser. The spectral resolution was 4 cm^{-1} with 10% laser

power and 10 s of exposure time along with a total of 15 acquisitions. The curves of the Raman shift between 800 and 1800 cm^{-1} were fitted using the version 4.1 of the XPSPEAK Software (Hong Kong).

RESULTS AND DISCUSSION

XRD Analysis for WP and Derived Biochars

XRD is used to study the short-range ordered structures and the crystalline structure of minerals in biochars. The XRD spectrograms of WP, CWB, and CWH are shown in Fig. 2. It can be concluded that main minerals in the biochars were calcite, hematite, rutile, iron monosulfide (FeS), and ferrosoferric oxide (Fe_3O_4) (Fan *et al.* 2015). The strong absorption of the diffraction peak intensity at 29.3° indicates a high content of calcite in biochars.

Two narrow and sharp peaks at 16° (101) and 22° (002) for WP were assigned to the crystalline region of cellulose. Compared to WP, the peak (002) of biochars became flatter and broader and the peak (101) vanished, indicating that the crystalline cellulose was totally destroyed during char formation and the structure of biochars was virtually amorphous. The peak (002) value shifted from 22° to 22.8°, indicating the development of atomic order in the carbonized material. This peak comes from the formation and successive ordering of aromatic structures, indicating crystallization and an increase in crystallinity. The formation of aromatic structures began after the complete decomposition of the wood nano-composite structure during the charring process (Paris *et al*. 2005). Peaks at 26.6° were not seen in the XRD spectrograms, which illustrated that biochars are not graphitized at 500 °C. As can be seen in Fig. 2, there was no remarkable difference between CWB and CWH.

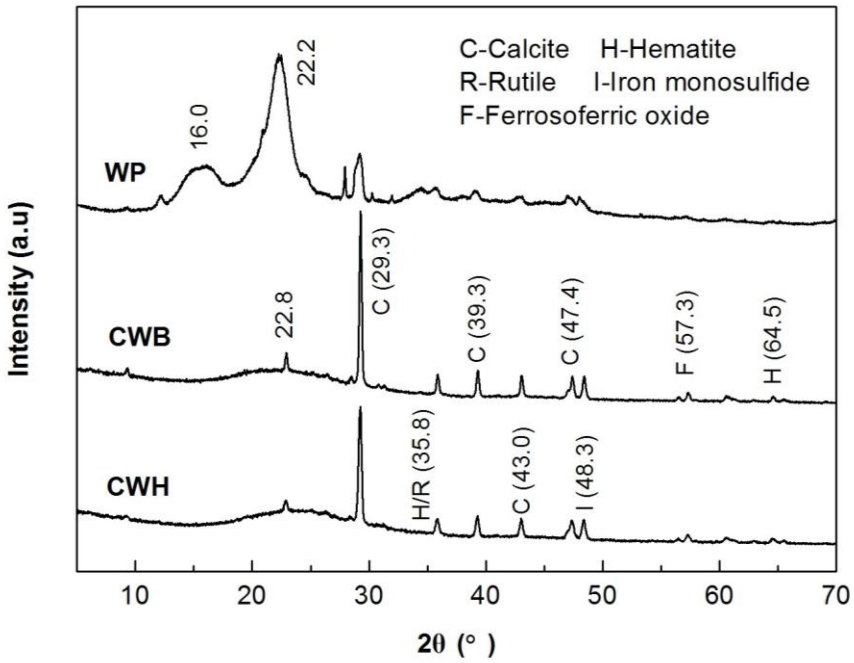

Fig. 2. XRD spectrograms for WP and its derived biochars

TG Analysis of WP and Derived Biochars

Thermogravimetric (TG) and differential thermogravimetric (DTG) curves for WP and derived biochars are shown in Fig. 3. Weight loss of WP up to 120 °C was due to water releasing from the raw material, indicating that the moisture content of WP was approximately 6.5%. The WP degradation at 212 to 430 °C was caused by the pyrolysis of hemicellulose (200 to 300 °C), cellulose (300 to 400 °C), and lignin (200 to 700 °C) (Gronli *et al.* 2002). The DTG curve of CWB exhibited a hump at 360 to 745 °C because of the degradation of cellulose, lignin at 360 to 640 °C, and thermal decomposition of calcite at 667 to 745 °C, which indicates that the CWB consisted of cellulose, lignin, and minerals. The DTG curve of CWH had only one peak, at 711 to 781 °C, caused by calcite decomposition, and a slight slope caused by lignin degradation at 400 to 660 °C, which indicates that the CWH consisted of lignin and minerals. The CWH had higher residue, of 52.8%, at 800 °C compared to CWB. It can be concluded that the CWH was more completely degraded than CWB.

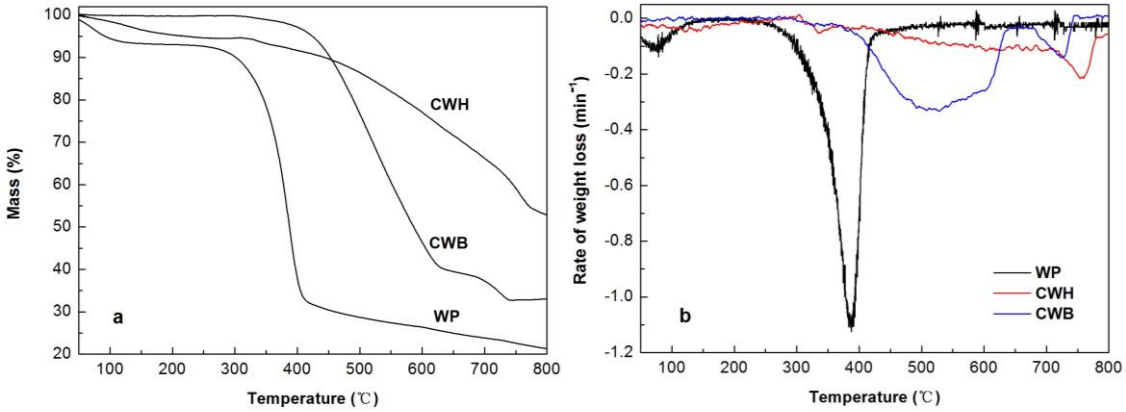

Fig. 3. The (a) thermal gravimetric and (b) differential thermal gravimetric curves for WP and its derived biochars

XPS Analysis of Biochars

XPS is an effective characterization technique for determining the qualitative and quantitative information for chemical elements (except hydrogen and helium) and chemical functional groups on solid surfaces.

XPS with survey scan mode was performed for biochars to identify and quantify their basic elements, as seen in Fig. 4 and Table 1. The results showed that the surface chemicals of biochars mainly consist of C, O, and Ca, which is in good agreement with XRD analysis. As seen in Table 1, CWH had a lower O/C ratio than CWB. The O/C ratio of WP is primarily determined by the content of hemicellulose and lignin. The hemicelluloses of biochars were degraded completely at 500 °C, so the decreasing O/C ratio of CWH could be attributed to lignin regeneration, which can be confirmed from the TG analysis results.

XPS with C1s region scan mode was performed for biochars to identify and quantify chemical functional groups, as can be seen in Fig. 5. The functional groups of biochars were classified as shown in Table 1 (C1, C2, C3, C4 were assigned to C=C/C-C/CHx, -C-OR, C=O, and –COO, respectively). The results showed that CWH has higher C1 content and lower C2, C3, and C4 contents compared to CWB, indicating that the number of oxygen-containing groups on the surface of CWH is lower than that on CWB.

The oxygen-containing acidic functional groups of biochar play a negligible role in sorption (Srinivasan *et al.* 2014). Therefore, CWH with lower content of oxygen-containing groups is more effective in sorbing organic and inorganic compound as a soil adsorbent than CWB. It also should be noted that the low numbers of oxygen-containing groups of biochar makes it profitable as a solid fuel.

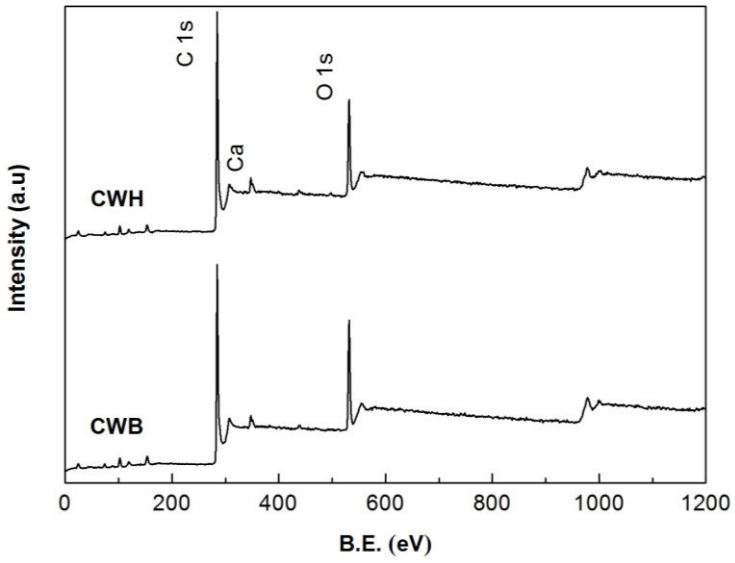

Fig. 4. XPS with survey scan mode for biochars

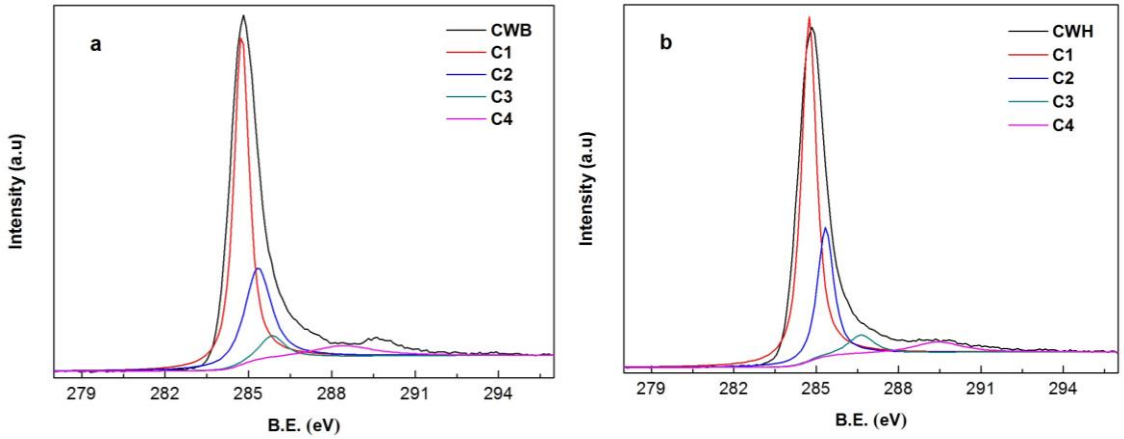

Fig. 5. C1s curve fitting for (a) CWB and (b) CWH

Table 1. Surface Chemical Components for Biochars

Biochar Samples	Atomic constitution (%)				C1s components (%)			
	C	O	N*	O/C	C1	C2	C3	C4
CWB	80.28	19.09	0.63	23.78	57.40	28.12	6.70	7.78
CWH	83.22	15.71	1.07	18.88	62.57	25.14	5.98	6.31

*calculated by difference

FT-IR Analysis for Biochars

The FT-IR spectra for biochars are shown in Fig. 6. The absorbance peak at 3420 cm^{-1} arises from the -OH of alcohols and phenols. It can be seen that the absorbance peaks at 1428, 1123, and 1022 cm^{-1} of CWH, which can be assigned to methoxyl (-OCH_3), ether (C-O-C), and alcohol (C-O), respectively, were lower compared to CWB, indicating that CWH had lower content of oxygen-containing groups (Islam *et al.* 2005). The absorbance peaks attributable to aromatic ring and unsaturated carbon (C-H, 2922 cm^{-1}), aliphatic carbon (C-H, 2851 cm^{-1}), and aromatic hydrogen (C-H, 877 cm^{-1}) in CWH were both lower than that of CWB, indicating that CWH was more completely degraded and has improved aromatic structure, which is in good agreement with the TG analysis. Peaks at 1628 cm^{-1} showed C=O axial deformation corresponding to various acids, aldehydes, and ketones (Vargas *et al.* 2011).

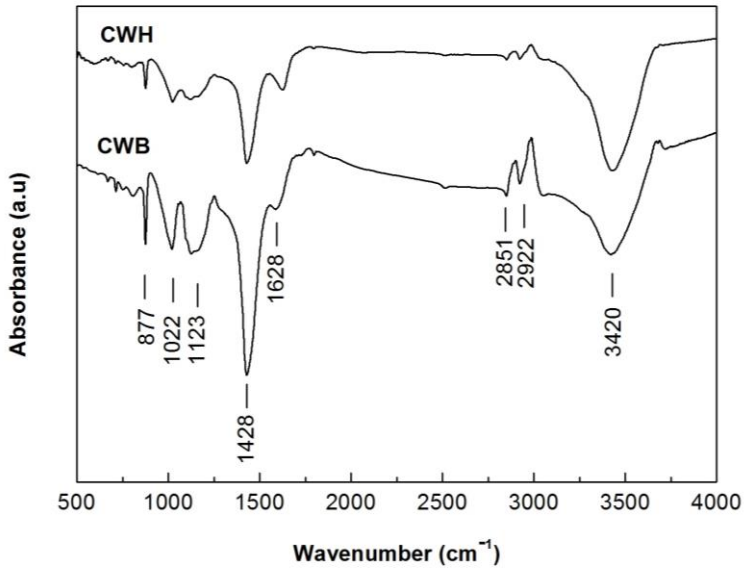

Fig. 6. FT-IR spectra for biochars

Thermochemical Properties of Raw Materials and Its Derived Biochars

The thermochemical properties of raw materials and derived biochars were determined as can be seen in Table 2. The elemental analysis results showed that the carbon density of derived biochars was increased dramatically and oxygen has been removed through the dehydration and volatilization. CWH had higher carbon content but lower oxygen content and char yield as compared to CWB, which is related to reacted hydrogen transferring from polyethylene chain to WP-derived radicals resulting in secondary crack on WP-derived char (Ren *et al.* 2009; Oyedun *et al.* 2014). The decrease of O/C in CWH as compared to CWB implied that more aromatic carbon structures were formed in biochar. Moisture content in WP (6.5 wt.%) is close to lignocellulose materials and relatively lower than goat manure and swine solids (8.7 wt.% and 13.6 wt.%, respectively) (Hsu and Lo 2001; Touray *et al.* 2014). It should be noted that low moisture content in feedstock will permit its rapid thermochemical conversion. Ash content in WP is relatively lower than rice-related residues and poultry manure, whereas it is higher than those contents in common biomass, *e.g.* sawdust and switch grass (Giron *et al.* 2013; Wanapeera *et al.* 2012; Zhang *et al.* 2015). Calorific value (CV) and fuel ratio (FR) were

considered as important fuel-related properties determining the rank of any biomass fuel (Touray *et al.* 2014).

As can be seen in Table 2, the CV and FR of WP were 14.57 kJ/g and 0.13 respectively, higher than poultry manure (11 to 14 kJ/g) but lower than crop residues (15 to 20 kJ/g) (Wang *et al.* 2011; Cantrell *et al.* 2012). These differences were mainly related to high ash content in WP (11.2 wt.%). Each 1% of increasing ash content will lead to a decrease of about 0.2 kJ/g in the calorific value (Jenkins *et al.* 1998). CWH had higher CV and FR as compared to CWB, which is attributed to higher carbon density and fixed carbon content in CWH. The CV of CWH was higher than biochars derived from poultry manure (*i.e.* 15.8 to 16.4 kJ/g of goat manure, 15.07 kJ/g of swine solids, and 13.5 kJ/g of chicken manure) (Cantrell *et al.* 2008, 2012), while very much lower than fossil coal (28.0 to 32.0 kJ/g) (Wolela 2007).

Table 2. Thermochemical Properties for Raw Materials and Its Derived Biochars

Thermochemical properties	WP	HDPE	CWB	CWH	Increment[e]
Elemental analysis[a] (wt.%)					
C	39.78	85.43	59.00	63.81	8.14
H	5.50	14.21	2.10	2.38	13.33
O[b]	54.62	0.15	38.88	33.78	-13.12
N	0.10	0.08	0.02	0.03	-
H/C molar ratio	1.66	1.99	0.43	0.45	4.65
O/C molar ratio	1.03	0.001	0.49	0.40	18.37
Proximate analysis (wt.%)					
Volatile	72.8	100	22.7	15.2	-33.04
Moisture	6.5	-	1.1	1.1	-
Ash	11.2	-	42.1	46.8	11.16
Fixed carbon[b]	9.5	-	34.1	36.9	8.21
Fuel properties					
Yield[c] (wt.%)	-	-	33.5	24.2	-27.76
Calorific value[c] (kJ/g)	14.57	38.66	17.62	21.68	23.04
Fuel ratio[d]	0.13	-	1.50	2.42	61.33

a Dry basis and ash-free
b Calculated by difference.
c Dry basis.
d Calculated as the ratio of fixed carbon to volatile matter.
e Calculated by the formula: (CWH-CWB)/CWB.

SEM for Morphology Analysis of Biochars

The morphological micrographs of WP, CWB, and CWH are shown in Fig. 7. WP is composed by massive fibrous materials with rough surface (Fig. 7a and Fig. 7b). Due to the dehydration and volatilization of raw materials, a small amount of pores with different sizes appeared in both CWB and CWH, and the edge of those biochars became bent after pyrolysis. These effects are highlighted with red ellipses and rectangles in Fig. 7c and Fig. 7d. CWH had smaller pore sizes as compared to CWB, and its surface exhibited obvious stratification. Those observations are related to the HDPE secondary cracking effect (Ren *et al.* 2009; Oyedun *et al.* 2014) and are highlighted with red squares in Fig. 7c and Fig. 7d.

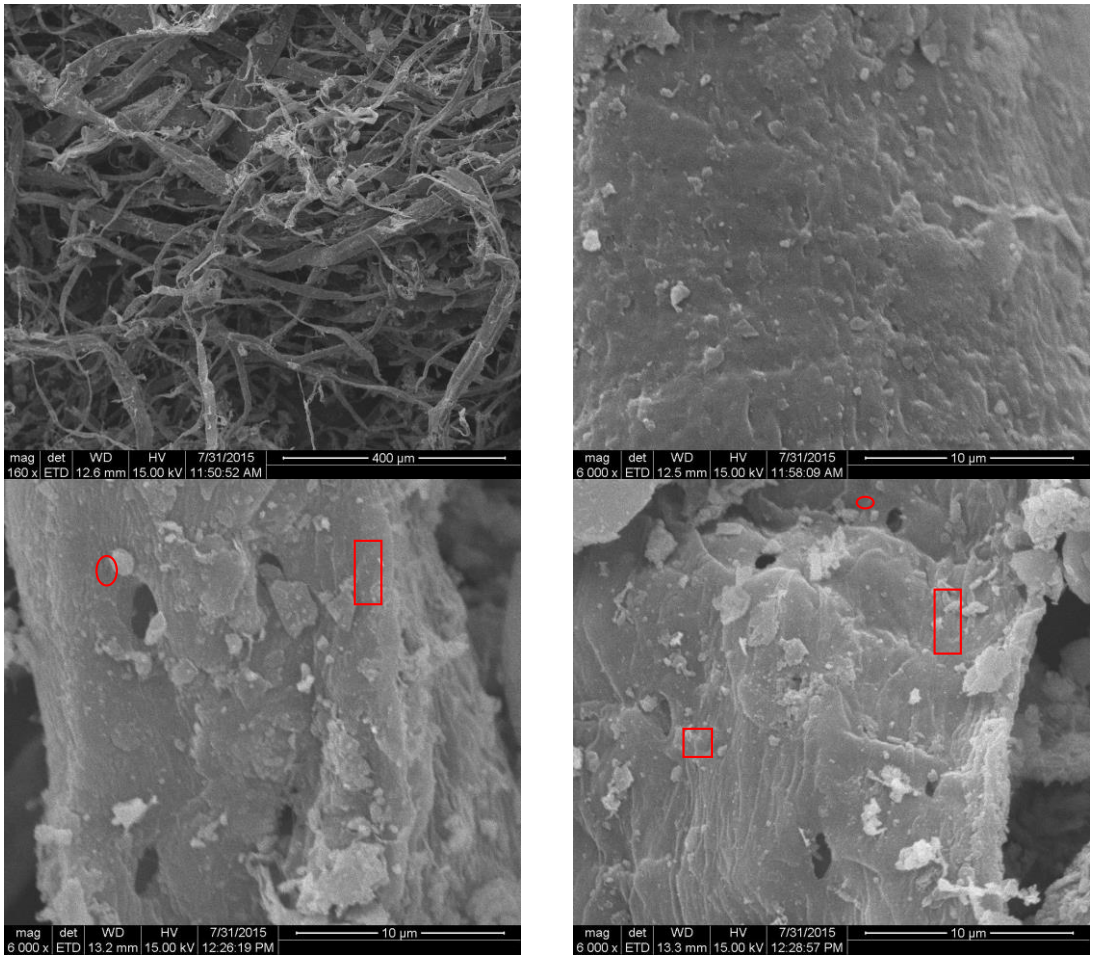

Fig. 7. SEM micrographs of (a) WP, 160× magnification, (b) WP, 6000× magnification, (C) CWB, 6000× magnification, (d) CWH, 6000× magnification

Surface Area and Pore Analysis for Biochars

The nitrogen adsorption isotherms and pore size distributions of CWB and CWH are presented in Figs. 8 and 9, respectively. According to the BDDT classification system, the N_2 adsorption isotherms of both CWB and CWH (Fig. 8) exhibited the type IV isotherm curves. A slight increment in adsorption amount at the low relative pressure region and a sharp increment at the relative pressure near 1 imply a poor microporosity development in the CWB and CWH (Mohan *et al.* 2014). The amount of absorbed volume increased gradually within the relative pressure region of 0.2 to 0.8, reflecting the presence of mesopores with a broad distribution (Wang *et al.* 2014; Mohan *et al.* 2014). The pore size distribution in CWH and CWB (Fig. 9) do not display a complete distribution near the lower pore size limit, which indicates the existence of micropores. The micropores distribution curve inserted in Fig. 8 shows that the micropores distributions of CWH and CWB were centered at 0.97 and 1.10 nm. No peaks appeared within the pore diameter region of 2 to 180 nm, and the BJH pore distribution curves exhibited a rapidly decreasing straight slope, indicating a broad pore diameter distribution (Li *et al.* 2010). From Figs. 8 and 9, it can be concluded that the degree of porosity development in CWH was remarkably greater than that in CWB (Mohan *et al.* 2014).

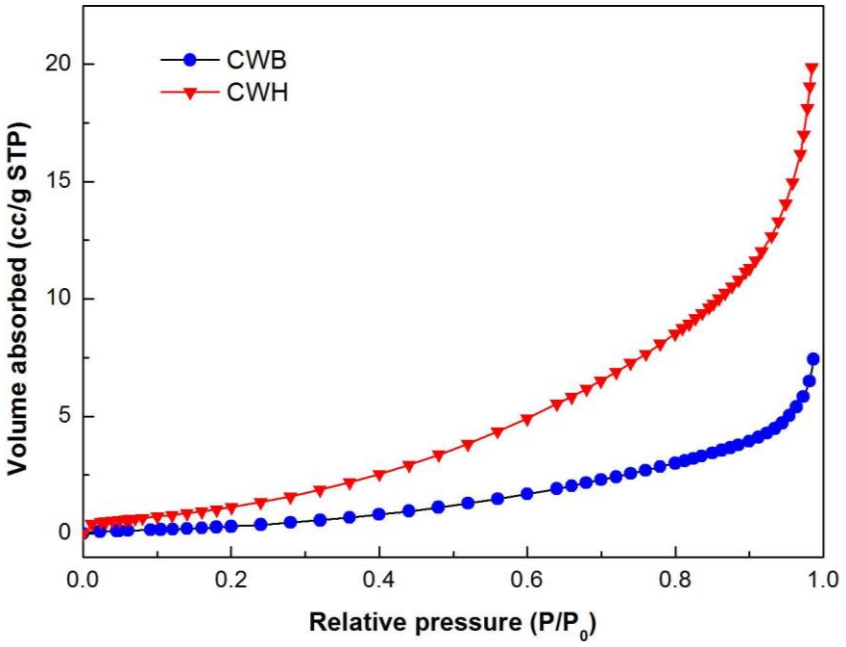

Fig. 8. Adsorption isotherms for N_2 at 77 K for biochars

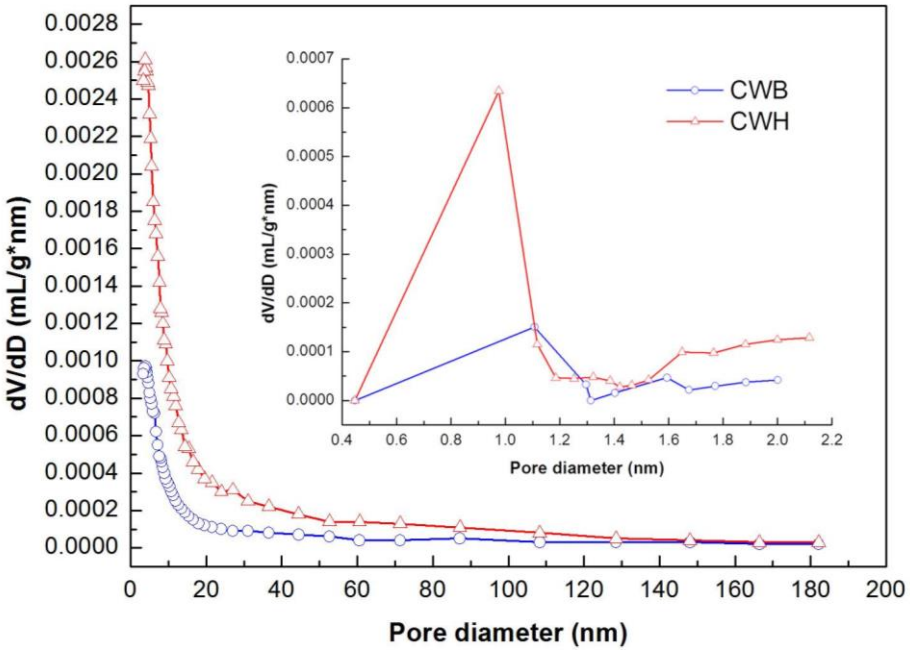

Fig. 9. The pore size distribution of biochars
Note: All curves in Fig. 8 were based on adsorption isotherms.

BET surface area and pore properties of CWB and CWH are shown in Table 3. Due to the HDPE secondary cracking effect on CWH, more volatile matter escaped and more pores were formed, which led to BET surface area and total pore volume of CWH remarkably higher than CWB. Moreover, CWH had relatively higher BET surface area (13.6 m^2/g) as compared to biochars obtained from goat manure, swine solids, and tea-leaves (1.7, 3.9, and 6.2 to 11.5 m^2/g, respectively) (Tsai *et al.* 2012; Peng *et al.* 2013;

Touray *et al.* 2014), whereas CWH had lower BET surface area than biochar obtained from sewage sludge (24.53 m^2/g) (Yuan *et al.* 2015) at the some pyrolysis temperature. CWH had remarkably lower average pore width as compared to CWB. This was related to the stratifying effect as seen in SEM, leading to the shrinkage of some of the larger macropores.

Table 3. BET Surface Area and Pore Properties of Biochars

Sample	BET surface area (m^2/g)	Total pore volume (cm^3/g)	Average pore width[f] (nm)	Micropore volume[g] (cm^3/g)
CWB	4.521	0.0299	26.49	0.0045
CWH	13.598	0.0587	17.26	0.0096

f Calculated from BET surface area and total pore volume.
g Calculated by the *t*-plot method.
Note: All data in Table 3 were calculated from adsorption isotherm.

Raman Analysis for Biochars

Raman spectroscopy can be used to characterize the aromaticity of biochars because of its high sensitivity toward the amorphous carbon structure. Raman spectra for biochars in the range of 800 to 1800 cm^{-1} are shown in Fig. 10, which were deconvoluted using Raman WIRE software to a maximum seven pseudo-bands in Gaussian mode (Li *et al.* 2006). It can be seen that four curves are fitted in Fig. 7, assigned to I_D, I_G, I_S, and I_O. I_D (1328 cm^{-1}) and I_G (1573 cm^{-1}) are the two main bands typically observed for biochars, which can be assigned to polyaromatic and graphitic carbons, respectively (Guerrero *et al.* 2008). The I_D (defect) band can be assigned to C-C between aromatic (benzene) rings, which shows the presence of medium to large aromatic rings including six or more fused rings and the existence of graphitic lattice without special order (Asadullah *et al.* 2010; Fuertes *et al.* 2010). The I_G (graphite) band can be assigned to alkene C=C (aromatic ring quadrant breathing), which shows the presence of graphitic bands and ideal graphitic lattice.

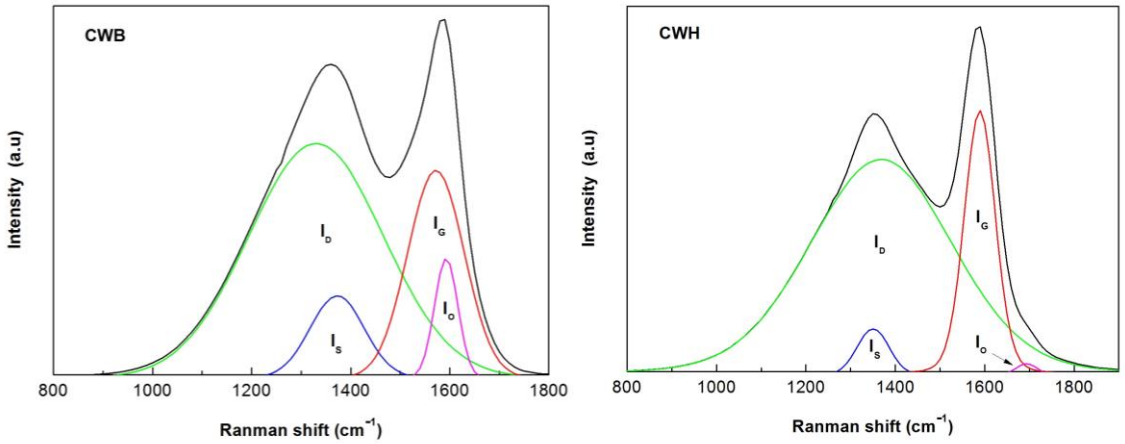

Fig. 10. Raman spectral curve fitting for biochars

As can be seen in Fig. 7, the I_D and I_G bands of biochars were broader compared to the sharp and distinct shapes of highly ordered carbon materials such as graphite

because of the presence of oxygen and various types of aliphatic compounds (Keown *et al.* 2007). The band area ratio between I_D and I_G (I_D/I_G) of CWH (3.75) was higher as compared to that of CWB (2.70), indicating a severe and effective structural change in biochar caused by enlargement of aromatic rings and the formation of a highly compact aromatic structure.

I_S (1374 cm^{-1}) can be assigned to the C-C structure of alkyl-aryl and methyl carbons connected to aromatic rings. I_O can be assigned to the carbonyl (C=O) structure. It can be concluded that the areas of I_O for CWH are far smaller than those for CWB, which can be attributed to the lower content of oxygen-containing groups such as carbonyl (C=O) in CWH, as confirmed by XPS and FT-IR analysis.

CONCLUSIONS

1. Biochar obtained by co-pyrolysis of waste newspaper (WP) with high-density polyethylene (HDPE) (CWH) has lower contents of oxygen-containing groups and increased aromatic structure as compared to WP-derived biochar (CWB).
2. HDPE secondary cracking effect caused CWH thermal degraded more completely as compared to CWB.
3. CWH has higher calorific value and fuel ratio than WP-derived biochar due to its higher carbon density and fixed carbon content.
4. Both CWH and CWB have poor porosity development and broad pore distribution. Moreover, CWH has greater porosity development as compared to CWB.
5. CWH is more appropriate as solid fuel, soil adsorbent or activated carbon precursor than CWB due to its lower oxygen-containing groups, increased aromatic structure, higher calorific value, higher fuel ratio, and greater porosity development.

ACKNOWLEDGMENTS

The authors are grateful for the support by the National Natural Science Foundation of China (Grant Nos. 31400515 and 31270606) and the Priority Academic Program Development of Jiangsu Higher Education Institutions (PAPD). Also, this paper was sponsored by the Qing Lan Project.

REFERENCES CITED

Achilias, D. S., Roupakias, C., Megalokonomos, P., Lappas, A. A., and Antonakou, E. V. (2007). "Chemical recycling of plastic wastes made from polyethylene (LDPE and HDPE) and polypropylene (PP)," *Journal of Hazardous Materials* 149(3), 536-542. DOI: 10.1016/j.jhazmat.2007.06.076

Ahmetli, G., Kocaman, S., Ozaytekin, I., and Bozkurt, P. (2004). "Epoxy composites based on inexpensive char filler obtained from plastic waste and natural resources," *Polymer Composites* 34(4), 500-509. DOI: 10.1002/pc.22452

Asadullah, M., Zhang, S., and Li, C. Z. (2010). "Evaluation of structural features of chars from pyrolysis of biomass of different particle sizes," *Fuel Processing Technology* 91(8), 877-881. DOI: 10.1016/j.fuproc.2009.08.008

Bornermann, L. C., Kookana, R. S., and Welp, G. (2007). "Differential sorption behaviour of aromatic hydrocarbons on charcoals prepared at different temperatures from grass and wood," *Chemosphere* 67(5), 1033-1042. DOI: 10.1016/j.chemosphere.2006.10.052

Cantrell, K. B., Ducey, T., Ro, K. S., and Hunt, P. G. (2008). "Livestock waste-to-bioenergy generation opportunities," *Bioresource Technology* 99(17), 7941-7953. DOI: 10.1016/j.biortech.2008.02.061

Cantrell, K. B., Hunt, P. G., Uchimiya, M., Novak, J. M., and Ro, K. S. (2012). "Impact of pyrolysis temperature and manure source on physicochemical characteristics of biochar," *Bioresource Technology* 107, 419-428. DOI: 10.1016/j.biortech.2011.11.084

Czernik, S., and Bridgwater, A. V. (2004). "Overview of applications of biomass fast pyrolysis oil," *Energy & Fuels* 18(2), 590-598. DOI: 10.1021/ef034067u

Fan, C., Yan, J. W., Huang, Y. R., Han, X. X., and Jiang, X. M. (2015). "XRD and TG-FTIR study of the effect of mineral matrix on the pyrolysis and combustion of organic matter in shale char," *Fuel* 139, 502-510. DOI: 10.1016/j.fuel.2014.09.021

Fuertes, A. B., Arbestain, M. C., Sevilla, M., Macia-Agullo, J. A., Fiol, S., Lopez, R. Smernik, R. J., Aitkenhead, W. P., Arce, F., and Macias, F. (2010). "Chemical and structural properties of carbonaceous products obtained by pyrolysis and hydrothermal carbonisation of corn stover," *Australian Journal of Soil Research* 48(6-7), 618-626. DOI: 10.1071/SR10010

Giron, R. P., Ruiz, B., Fuente, E., Gil, R. R., and Suarez-Ruiz, I. (2013). "Properties of fly ash from forest biomass combustion," *Fuel* 114, 71-77. DOI: 10.1016/j.fuel.2012.04.042

Guerrero, M., Ruiz, M. P., Millera, A., Alzueta, M. U., and Bilbao, R. (2008). "Characterization of biomass chars formed under different devolatilization conditions: Differences between rice husk and eucalyptus," *Energy & Fuels* 22(2), 1275-1284. DOI: 10.1021/ef7005589

Gronli, M. G., Varhegyi, G., and Di, B. C. (2002). "Thermogravimetric analysis and devolatilization kinetics of wood," *Industrial & Engineering Chemistry Research* 41(17), 4201-4208. DOI: 10.1021/ie0201157

Hsu, J. H., and Lo, S. L. (2001). "Effect of composting on characterization and leaching of copper, manganese, and zinc from swine manure," *Environmental Pollution* 114(1), 119-127. DOI: 10.1016/S0269-7491(00)00198-6

Islam, M. N., Islam, M. N., Beg, M. R. A., and Islam, M. R. (2005). "Pyrolytic oil from fixed bed pyrolysis of municipal solid waste and its characterization," *Renewable Energy* 30(3), 413-420. DOI: 10.1016/j.renene.2004.05.002

Jenkins, B. M., Baxter, L. L., and Miles, T. R. (1998). "Combustion properties of biomass," *Fuel Processing Technology* 54, 17-46.

Keown, D. M., Li, X. J., Hayashi, J. L., and Li, C. Z. (2007). "Characterization of the structural features of char from the pyrolysis of cane trash using Fourier transform-Raman spectroscopy," *Energy & Fuels* 21(3), 1816-1821. DOI: 10.1021/ef070049r

Li, X. L., Han, C. L., Chen, X. Y., and Shi, C. W (2010). "Preparation and performance of straw based activated carbon for supercapacitor in non-aqueous electrolytes,"

Microporous and Mesoporous Materials 131(1-3), 303-309. DOI: 10.1016/j.micromeso.2010.01.007

Li, X. J., Hayashi, J., and Li, C. Z. (2006). "FT-Raman spectroscopic study of the evolution of char structure during the pyrolysis of a Victorian brown coal," *Fuel* 85, 1700-1707. DOI: 10.1016/j.fuel.2006.03.008

Mckendry, P. (2002). "Energy production from biomass (part 2): Conversion technologies," *Bioresource Technology* 83(1), 47-54. DOI: 10.1016/S0960-8524(01)00119-5

Mohan, D., Kumar, H., Sarswat, A., Alexandre-Franco, M., and Pittman, C. U. (2014). "Cadmium and lead remediation using magnetic oak wood and oak bark fast pyrolysis bio-chars," *Chemical Engineering Journal* 236, 513-528. DOI: 10.1016/j.cej.2013.09.057

Mohan, D., Pittman, C. U., and Steele, P. H. (2006). "Pyrolysis of wood/biomass for bio-oil: A critical review," *Energy & Fuels* 20(3), 848-889. DOI: 10.1021/ef0502397

Oyedun, A. O., Tee, C. Z., Hanson, S., and Hui, C. W. (2014). "Thermogravimetric analysis of the pyrolysis characteristics and kinetics of plastics and biomass blends," *Fuel Processing Technology* 128, 471-481. DOI: 10.1016/j.fuproc.2014.08.010

Paris, O., Zollfrank, C., and Zickler, G. A. (2005). "Decomposition and carbonisation of wood biopolymers - A microstructural study of softwood pyrolysis," *Carbon* 43(1), 53-66. DOI: 10.1016/j.carbon.2004.08.034

Peng, C., Yan, X. B., Wang, R. T., Lang, J. W., Ou, Y. J., and Xue, Q. J. (2013). "Promising activated carbons derived from waste tea-leaves and their application in high performance supercapacitors electrodes," *Electrochimica Acta* 87, 401-408. DOI: 10.1016/j.electacta.2012.09.082

Ren, Q. Q., Zhao, C. S., Wu, X., Liang, C., Chen, X. P., Shen, J. Z., Tang, G. Y., and Wang, Y. (2009). "TG-FTIR study on co-pyrolysis of municipal solid waste with biomass," *Bioresource Technology* 100(17), 4054-4057. DOI: 10.1016/j.biortech.2009.03.038

Rotliwala, Y. C., and Parikh, P. A. (2011). "Thermal degradation of rice-bran with high density polyethylene: A kinetic study," *Korean Journal of Chemical Engineering* 28(3), 788-792. DOI: 10.1007/s11814-010-0414-1

Srinivasan, P., Sarmah, A. K., and Manley-Harris, M. (2014). "Sorption of selected veterinary antibiotics onto dairy farming soils of contrasting nature," *Science of the Total Environment* 472, 695-703. DOI: 10.1016/j.scitotenv.2013.11.104

Steinbeiss, S., and Gleixner, G. (2009). "Effect of biochar amendment on soil carbon balance and soil microbial activity," *Soil Biology & Biochemistry* 41(6), 1301-1310. DOI: 10.1016/j.soilbio.2009.03.016

Suelves, I., Lazaro, M. J., and Moliner, R. (2002). "Synergetic effects in the co-pyrolysis of samca coal and a model aliphatic compound studied by analytical pyrolysis," *Journal of Analytical and Applied Pyrolysis* 65(2), 197-206. DOI: 10.1016/S0165-2370(01)00194-2

Sutton, D., Kelleher, B., and Ross, J. R. H. (2001). "Review of literature on catalysts for biomass gasification," *Fuel Processing Technology* 73(3), 155-173. DOI: 10.1016/S0378-3820(01)00208-9

Touray, N., Tsai, W. T., Chen, H. R., and Liu, S. C. (2014). "Thermochemical and pore properties of goat-manure-derived biochars prepared from different pyrolysis temperatures," *Journal of Analytical and Applied Pyrolysis* 109, 116-122. DOI: 10.1016/j.jaap.2014.07.004

Tsai, W. T., Liu, S. C., Chen, H. R., Chang, Y. M., and Tsai, Y. L. (2012). "Textural and chemical properties of swine-manure-derived biochar pertinent to its potential use as a soil amendment," *Chemosphere* 89(2), 198-203. DOI: 10.1016/j.jaap.2015.01.010

Vargas, A. M. M., Cazetta, A. L., Garcia, C. A., Moraes, J. C. G., Nogami, E. M., Lenzi, E., Costa, W. F., and Almeida, V. C. (2011). "Preparation and characterization of activated carbon from a new raw lignocellulosic material: Flamboyant (*Delonix regia*) pods," *Journal of Environmental Management* 92(1), 178-184. DOI: 10.1016/j.jenvman.2010.09.013

Vasile, C., and Brebu, M. A. (2006). "Thermal valorisation of biomass and of synthetic polymer waste. Upgrading of pyrolysis oils," *Cellulose Chemistry and Technology* 40(7), 489-512.

Wanapeera, J., Li, X., Worasuwannarak, N., Ashida, R., and Miura, K. (2012). "Production of high-grade carbonaceous materials and fuel having similar chemical and physical properties from various types of biomass by degradative solvent extraction," *Energy & Fuels* 26(7), 4521-4531. DOI: 10.1021/ef3003153

Wang, L. J., Shahbazi, A., and Hanna, M. A. (2011). "Characterization of corn stover, distiller grains and cattle manure for thermochemical conversion," *Biomass & Bioenergy* 35(1), 171-178. DOI: 10.1016/j.biombioe.2010.08.018

Wang, Q., Yan, J., Wang, Y. B., Wei, T., Zhang, M. L., Jing, X. Y., and Fan, Z. J. (2014). "Three-dimensional flower-like and hierarchical porous carbon materials as high-rate performance electrodes for supercapacitors," *Carbon* 67, 119-127. DOI: 10.1016/j.carbon.2013.09.070

Wolela, A. (2007). "Fossil fuel energy resources of Ethiopia: Coal deposits," *International Journal of Coal Geology* 72(3-4), 293-314. DOI: 10.1016/j.coal.2007.02.006

Yu, J. S., Zhao, Y. C., and Li, Y. D. (2014). "Utilization of corn cob biochar in a direct carbon fuel cell," *Journal of Power Sources* 270, 312-317. DOI: 10.1016/j.jpowsour.2014.07.125

Yuan, H. R., Lu, T., Huang, H. Y., Zhao, D. D., Kobayashi, N., and Chen, Y. (2015). "Influence of pyrolysis temperature on physical and chemical properties of biochar made from sewage sludge," *Journal of Analytical and Applied Pyrolysis* 112, 284-289. DOI: 10.1016/j.jaap.2015.01.010

Zhang, Y., Zhai, M., Wang, X. Y., Sun, J. W., Dong, P., Liu, P. B., and Zhu, Q. Y. (2015). "Preparation and Characteristics of Biomass Char," *Bioresources* 10(2), 3017-3026.

Article submitted: April 13, 2015; Peer review completed: July 20, 2015; Revised version received and accepted: October 12, 2015; Published: October 27, 2015.
DOI: 10.15376/biores.10.4.8253-8267